Journal of Alloys and Compounds 785 (2019) 13–18

Contents lists available at ScienceDirect

Journal of Alloys and Compounds

journal homepage: http://www.elsevier.com/locate/jalcom

Influence of Ag doping on the dielectric and magnetic properties of $LiFe_5O_8$ ceramics

Keywords:
Spinel
Magnetic
Dielectric

A B S T R A C T

A novel spinel $Li_{1-x}Ag_xFe_5O_8$ ($0 \leq x < 0.2$) solid solution ceramics were fabricated via solid state reaction method. Based on XRD and SEM analysis, it was found that the spinel solid solution was formed in limited composition range. Both the dielectric and magnetic properties have been improved a lot, and the $Li_{0.95}Ag_{0.05}Fe_5O_8$ sample achieved the higher the real part of both permittivity and permeability as 170 and 47.1, respectively at 200 MHz and 20 MHz, which was attributed to the Ag^+ substitutions. Considering its dielectric and magnetic properties, the $Li_{1-x}Ag_xFe_5O_8$ ($0 \leq x < 0.2$) ceramics provide a way in developing multifunctional materials for multifunctional electronic devices applications.

1. Introduction

An advanced electromagnetic materials combined with a variety of functions have been studied to meet the need of information and wireless technologies with the rapid development of the electronic industry [1,2]. In recent years, among different kinds of functional ceramics materials, soft magnetic materials have been designed as a variety of forms in possession of high permittivity and permeability as well as the dielectric and magnetic loss tangents [3]. At the same time, some traditional ceramic materials still don't adapt to high frequency. Therefore, more and more attentions have been paid to the electromagnetic materials that are required to possess multifunctionality and work at high frequency [4,5].

Among the reported functional materials, the spinel ferrites possess excellent and unique performances such as high permittivity, low dielectric loss, and large saturation magnetization, so a number of researchers have concentrated on exploring the spinel ferrites further [6,7]. Generally speaking, with regards to the spinel ferrites, the structure of AB_2O_4 can be described as a normal cubic phase. However, the inverse spinel group structure, which formula is $B(AB)O_4$, can be composed of the octahedral sites doped with A sites and one half of B sites and the tetrahedral sites doped with the other half of B sites [8,9]. As far as the spinel structure is concerned, $LiFe_5O_8$, the potential cathode materials in lithium-ion batteries, which has also been considered as the components of microwave devices such as phase shifters, isolators, circulars, and gyrators, has been designed in a wide number of applications and electromagnetic materials [10]. Based on its special structure with Fe^{3+} occupying both A sites and B sites and Li^+ occupying the B sites, respectively, many researchers have paid more attention to modifying ions on both A and B sites [11]. Furthermore, the existing results have shown that it has namely two crystallographic phases, α-$LiFe_5O_8$ and β-$LiFe_5O_8$ that belong to the space group $P4_332$ and Fd-3m, respectively [12]. In the α-$LiFe_5O_8$ phase, the B sites ordered phase was occupied by the octahedral sites with Li^+ and Fe^{3+} ions. On the contrary, the β-$LiFe_5O_8$ belongs to a disordered structure, in which the ions were distributed randomly [13–16]. Generally, a closed-packed array of oxygen atoms with oxygen tetrahedron and octahedron has been composed of the disordered spinel structure. The reason of cation disordering and ordering in spinel structure are of great importance is that it has a wise influence in the physical properties [17].

In our previous work, it was found that $LiFe_5O_8$ and $Li_2ZnTi_3O_8$ can form solid solution in the whole composition range. Excellent dielectric and magnetic properties with permittivity ~19.6 and permeability ~38.2 were obtained in the $0.25LiFe_5O_8$-$0.75Li_2ZnTi_3O_8$ ceramics [18]. Furthermore, He et al. [19] also has done a series of researches on the low temperature co-fired magneto-dielectric $Li_2MoO_4/Ni_{0.5}Zn_{0.5}Fe_2O_4$ composites for high-frequency application, which concluded that the optimal sample ($x \leq 0.5$) possess both good and stable magneto-dielectric properties in the frequency range from 10 MHz to 1 GHz with acceptable good densities. Besides, Lin et al. [20], has revealed the fact that the laminated magneto-dielectric $Ni_{0.5}Ti_{0.5}NbO_4$-$Ni_{0.8}Zn_{0.2}Fe_2O_4$ composites possess excellent and stable magneto-dielectric properties in the frequency range from 10 MHz to 1 GHz, in which the 60% NTN - 40% NZO composites owned favorable permittivity and permeability of 34 and 9.12 at 10 MHz, respectively, as well as the ultra dielectric loss and magnetic loss of 0.03 and 0.16 respectively.

In this paper, considering the similar ionic radius, the same electrovalence and the good electrical conductivity, the Ag^+ is attempted to add into $LiFe_5O_8$ accompanied with entering the B sites, in order to obtain the uniform structure, the high permittivity and permeability, the ultra-low dielectric/magnetic loss, and the excellent saturation magnetization.

https://doi.org/10.1016/j.jallcom.2019.01.148
0925-8388/

2. Experimental

According to the ratio of the chemical of $Li_{1-x}Ag_xFe_5O_8$ (x = 0, 0.05, 0.1, 0.15, 0.16, 0.17, 0.18, 0.19), the proportionate amounts of the raw materials of Li_2CO_3(≥98.0%), Ag_2CO_3(≥98.0%), Fe_2O_3(≥99.0%; Sinopharm Chemical Reagent, Shanghai, China) were measured. Then, the reagent-grade starting materials were mixed and milled for 4 hours with the media of ethyl alcohol and ZrO_2 balls using a planetary mill. After being dried in the blast air oven, the powders mixture was pre-sintered at 900 °C for 3 hours with occurring to the solid-state reaction. Next, the calcined powders were milled again for 4 hours with the media of ethyl alcohol and ZrO_2 balls, which can obtain the homogeneous and fine powders. Similarly after being dried, the mixed powders were added to 5 wt % PVA and pressed to small cylinders (10 mm in diameter) and circular rings (9 mm in inner diameter and 15 mm in external diameter, respectively) through the powder pressing machine in order to form the dense compacts. With the temperature range from 1050 °C to 1250 °C, these cylinders and rings were sintered 2 hours with the heating ratio of 3 °C/min.

The crystal structures of the $Li_{1-x}Ag_xFe_5O_8$ materials were investigated by X-ray diffraction (XRD) in room temperature which used of CuKα radiation from 10 to 70° 2θ at a step size of 0.02°, 40 kV, and 100 mA (Rigaku D/MAX-2400 X-ray diffractometry, Tokyo, Japan). The microstructures of the sintered samples were observed on the ceramics surfaces by a scanning electron microscopy (SEM) (Helios G4 CX, FEI). The magnetic and dielectric properties were performed through using with the RF impedance analyzer HP 4291B through the 16454L and 16453 magnetic and dielectric material test fixture, independently. Meanwhile, the tested sample needs to be made as a small pellet with the diameter of 10 mm for dielectric performance, and similarly, for magnetic performance it needs to be made as the ring with about 7 mm inner diameter and 12 mm outer diameter. The magnetic hysteretic loop was investigated by vibrating sample magnetometer.

3. Results and discussions

Fig. 1 reveals XRD patterns of the $Li_{1-x}Ag_xFe_5O_8$ ($0 \le x < 0.2$) ceramics sintered at different optimum temperatures with 2θ from 10° to 70°. The XRD patterns show that the main phase is typical spinel phase in $Li_{1-x}Ag_xFe_5O_8$ compositions. According to the standard cubic spinel phase, the molecular formula of $LiFe_5O_8$ could be written as $Fe(Li_{0.5}Fe_{1.5})O_4$, which the O^{2-} arrange based on the rule of CCP (cubic close packing), including the tetrahedral site and the octahedral site [19]. Meanwhile, the two fifths Fe^{3+} occupy the A sites, thus the rest of Fe^{3+} take up the B sites accompanying with the Li^+. In addition, with the x value increases, the Ag^+ is introduced into the $LiFe_5O_8$ phase, therefore, the diffraction peaks of (111), (210), (211), (220), (310), (311), (400), (421), (422), (511), (440) appear indicating that there is an order process of ion destruction and reconstruction in these spinel ceramic samples. Furthermore, the major peaks move towards the small 2θ angle direction because of the increase of the cell parameters. In this figure, the red heart-shaped represent for the Ag phase according to compare with the standard phase card of pure Ag. Furthermore, the Li^+ at B sites are partly substituted by Ag^+, suggesting that the diffraction peaks of the $LiFe_5O_8$ have changed, such as the decrease of (311), (320) and (110).

The schematic diagram of the AB_2O_4 spinel structure is presented in Fig. 2a. In a general way, the olive color ions stand for Fe^{3+} at A sites, and the purple ions for B sites with three fifths Fe^{3+} and Li^+ accompanying with the red balls for all oxygen ions. Due to the Ag substitution, it is more likely to lead to a statistically disorder within the structure and disrupts the ordered arrangement of Li^+ and Fe^{3+} at the octahedral B sites, which is corresponding to the reduction of the superlattice X-ray diffraction peaks. At the same time, Fig. 2b shows the density and cell parameters of the $Li_{1-x}Ag_xFe_5O_8$ ($0 \le x < 0.2$) ceramics with the Ag content increasing. As for the bulk densities, taking advantage of Archimedes principle, a series of densities of ceramics have gotten by the laboratory electronic balance under room temperature and with the following computational formula:

$$\rho = \frac{A}{A - B}\rho_0 - \rho_L + \rho_L \quad (1)$$

where A and B are the weight at air and the medium about deionized water, respectively, in addition, ρ_0 and ρ_L stand for the density of assistant liquid and atmosphere.

In fact, with the increase of the sintering temperature, the densities of the $Li_{1-x}Ag_xFe_5O_8$ ($0 \le x < 0.2$) ceramics can present firstly a slight rise, and then be a little down. Generally speaking, all the

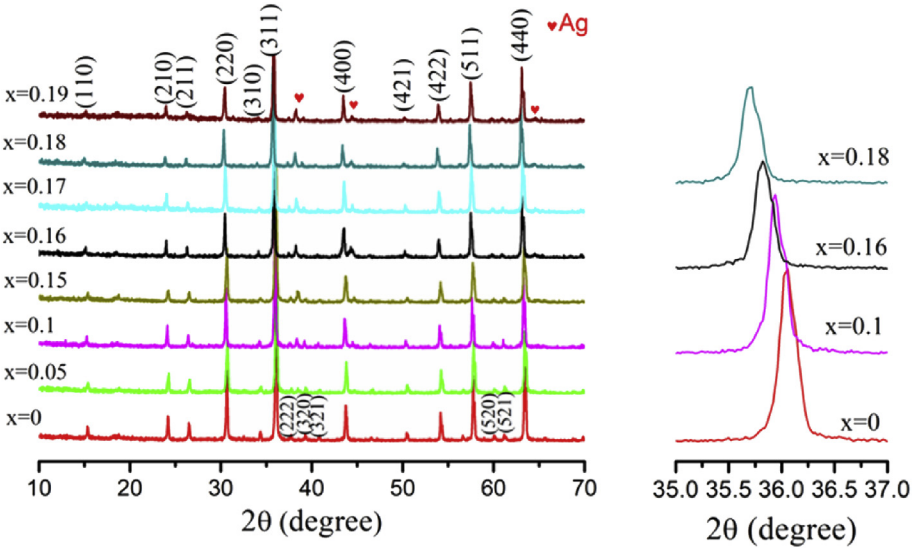

Fig. 1. X-ray diffraction patterns of the $Li_{1-x}Ag_xFe_5O_8$ ($0 \le x < 0.2$) ceramics sintered at different temperatures.

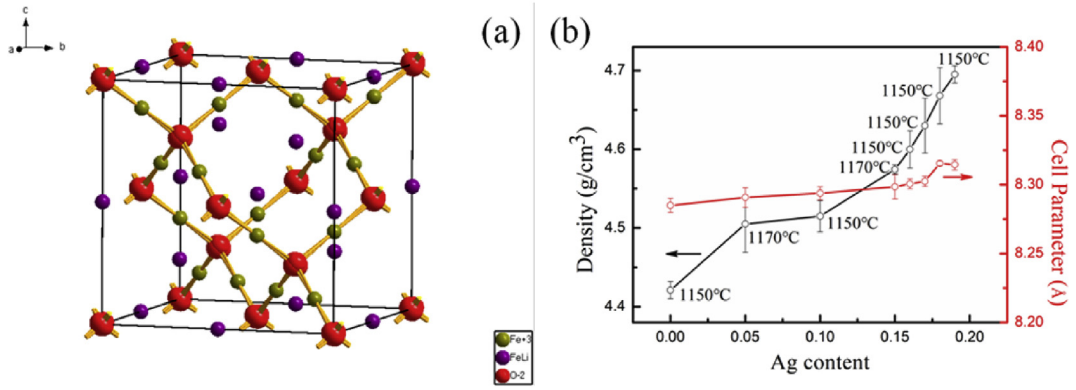

Fig. 2. Schematic diagram of the AB_2O_4 spinel structure (a), and the linear variation of the $Li_{1-x}Ag_xFe_5O_8$ ($0 \le x < 0.2$) ceramics in the cell parameters and densities as a function of composition (b).

materials possess this similar tendency of density vs. sintering temperature. At high temperature, secondary grain growth is popular in ceramics. As the content of Ag ion increases, the density of the $Li_{1-x}Ag_xFe_5O_8$ ceramics increase due to the larger molecular weight of Ag (107.8683 g/mol) than Li (6.941 g/mol). In particular, it is indicated that the densification temperature of the $Li_{0.95}Ag_{0.05}Fe_5O_8$ ceramic is around 1170 °C, with the temperature increasing, when the density of $Li_{0.95}Ag_{0.05}Fe_5O_8$ arrived at 4.672 g/cm^3. As can be seen from the picture, the cell parameters shows the linear variation matching with the phenomenon as shown in XRD pattern that the peaks moved towards small angle direction. Similarly, the cell parameters gradually increase with the increase of Ag content of ion due to the larger ionic radius of Ag^+ than Li^+. By means of the classic PDF cards about PDF#49-0266 and PDF#17-0114 that on behalf of the $Li_{0.5}Fe_{2.5}O_4$ and $LiFe_5O_8$ respectively, all cell parameters could be calculated as a function of x value. The average lattice constants of pure $LiFe_5O_8$ are calculated as $a = b = c = 8.284(9)$ Å, $\alpha = \beta = \gamma = 90°$, and $V_{unit} = 578.28$ Å^3.

Fig. 3 showed the surface morphology SEM micrographs of the typical $Li_{1-x}Ag_xFe_5O_8$ ceramics ($0 \le x < 0.2$) sintered at the optimum sintering temperature for 2 h. It can be easily seen that homogeneous and dense ceramic microstructure with a few pores can be observed from Fig. 3. As shown in the figure, however, with the increasing of the substitution Ag^+ content, the microstructure appeared the similarly layered structure and the average grain size decreased a little. Meanwhile, more and more distinct textured grain growth was observed, which should be related to its crystal structure.

The permittivity of the $Li_{1-x}Ag_xFe_5O_8$ ($0 \le x < 0.2$) ceramics as a function of the x value was revealed in Fig. 4. As shown in Fig. 4a, with the increase of Ag^+ doping, the real part of dielectric constant of the ceramics shows a considerable ascent. It is easily seen that when the chemical formula is $Li_{0.95}Ag_{0.05}Fe_5O_8$, the permittivity even reaches to the highest value 170 at about 200 MHz. Taken as a whole, the result presents that other formula of the $Li_{1-x}Ag_xFe_5O_8$ all appear a certain extent enhancement. For the ordinary spinel ferrites, the permittivity at 1 MHz among different compounds changes indicating that the permittivity can be significantly influenced by the electrical resistivity [21]. Therefore, it can be obviously seen from the change of the initial dielectric constant that the permittivity has been significantly influenced from the resistance of the material. Besides, in terms of spinel ferrites, the

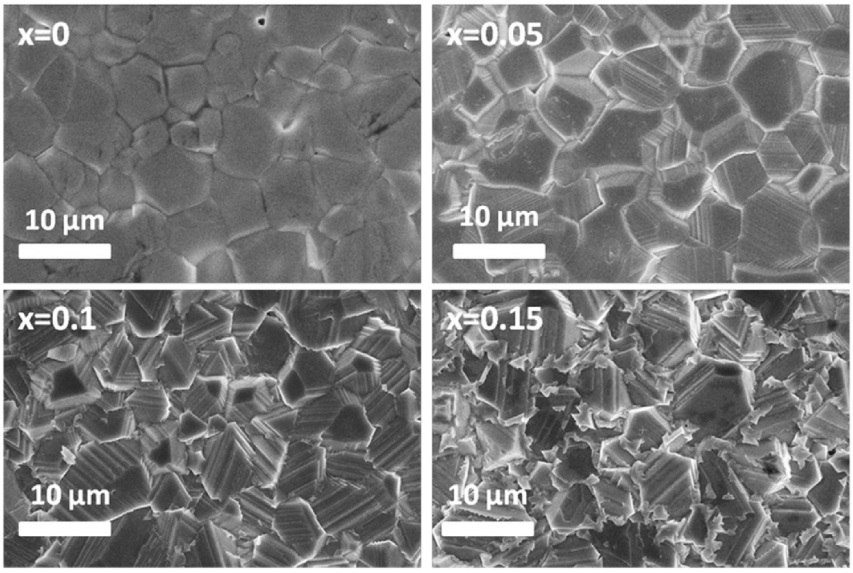

Fig. 3. The SEM micrographs of surfaces (x = 0, 0.05, 0.1, and 0.15) of the typical samples of $Li_{1-x}Ag_xFe_5O_8$ ($0 \le x < 0.2$) ceramics sintered at the optimum sintering temperature for 2 hours.

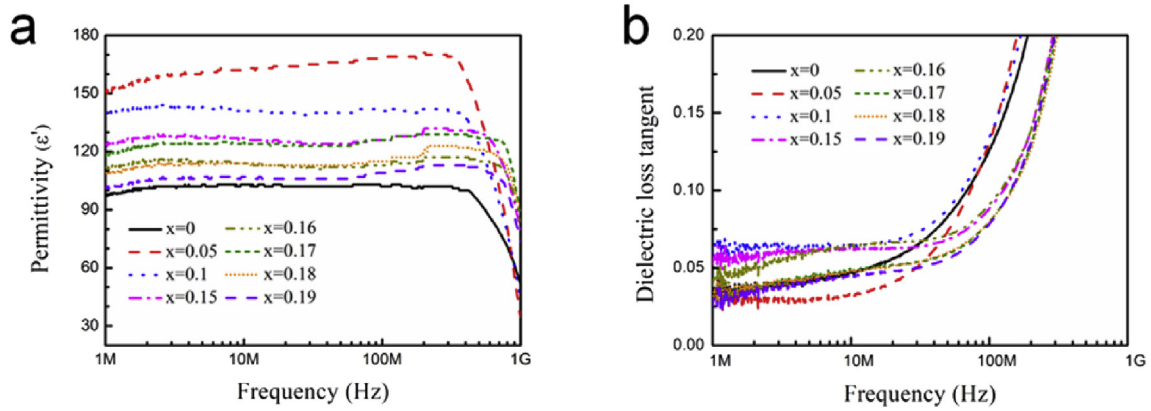

Fig. 4. Dielectric properties of the $Li_{1-x}Ag_xFe_5O_8$ ($0 \le x < 0.2$) ceramics as a function of the x value in the frequency range from 1 MHz to 1 GHz.

dielectric constant is usually expressed as relaxation-type dispersion, so that it shows a decrease trend in the high test frequency [22], which accounted for the phenomenon in Fig. 4a that the real part of the permittivity dropped abruptly at 200 MHz.

Likewise, as shown in Fig. 4b, it can be seen that the imaginary part of the permittivity about the $Li_{1-x}Ag_xFe_5O_8$ ($0 \le x < 0.2$) ceramics reveals an extremely low move towards, which is attributed to the doped Ag^+. Under the low frequency range, the dielectric loss tangents of a series of compounds reveal the ultra low numerical value, which was beneficial for the materials to attain the good physical performance. Furthermore, in other words, the lower the loss shows the better the material adapt to many occasion, which is the reason that the loss tangent is always required to possess the low value.

Fig. 5a presents the magnetic properties of the $Li_{1-x}Ag_xFe_5O_8$ ($0 \le x < 0.2$) ceramics with the change of x value in the frequency from 1 MHz to 1 GHz distinctly. It can be seen that the real part of permeability increases firstly and then decreases rapidly with the frequency going up, which seems a parabola going downwards. When x value equals to 0.05, the initial real part of the permeability reaches the maximum values about 47.1 at 20 MHz. Meanwhile, it can be easily concluded that a little Ag^+ doped is really attributed for improving the permeability of the spinel lithium iron oxide. Besides, the initial permeability should increase with x value adding, because the initial permeability of the lithium ferrite is strongly affected by magnetization saturation [23].

The initial permeability of the ferrites expresses an improvement with the increasing of the grain size, which also depends on the preparation technology. In addition, as the sintering temperature goes up, the initial permeability is increased at first and then decreased, on the contrary, the magnetic loss presents the different consequence [24]. It is well-known that the content of Fe^{3+} and the location of the doped ion in the crystal have influenced the ceramics' magnetic performance. Therefore, one of the main reasons about the change of ferrite materials is that the Ag^+ is doped into B sites, which results in the decline about the materials' permeability. What's more, the magnetic loss decreases firstly and then increases, and last decreases with the increasing of the frequency at Fig. 5b, which is attributed to the concentration of B sites ions [25].

The magnetic hysteretic loop of the $Li_{1-x}Ag_xFe_5O_8$ ($0 \le x < 0.2$) ceramics at room temperature in the magnetic field range of -4000-4000 Oe and -40-40 Oe are shown in Fig. 6a. In spinel ferrites, on the one hand, their magnetic moments are mainly given consideration to the uncompensated electron spins of the subjective ions and the spin alignments in the two sublattices which are not parallelly arranged. On the other hand, the other important factor that makes effect on the magnetic performance of ceramic materials is the location of the doped ions in the crystal. From the figure shows, it is obvious that the saturation magnetization is just a little lower than the standard sample when x value equals to 0.05, which is 62.01 emu/g. In most of the metal cations in spinel ferrite, the B sites ion is the most important factor about contributing to the magnetic properties of the ceramic materials [26,27]. Thus, it seems that a small amount of Ag^+ doped in B sites has decreased the saturation magnetization, and in this spinel AB_2O_4 ceramic, occupying the B sites ion is the main reason about the magnetic properties. As mentioned before, with the compositions,

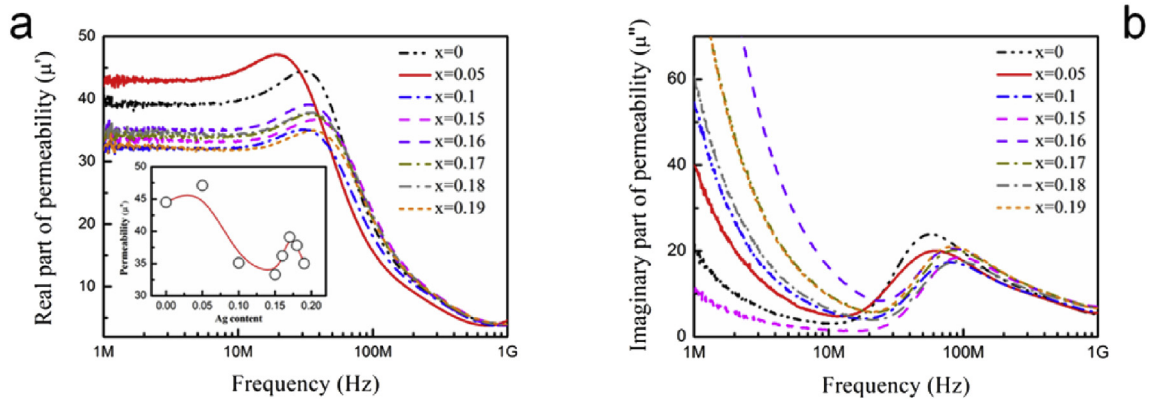

Fig. 5. Magnetic properties of the $Li_{1-x}Ag_xFe_5O_8$ ($0 \le x < 0.2$) ceramics as a function of x value in the frequency from 1 MHz to 1 GHz.

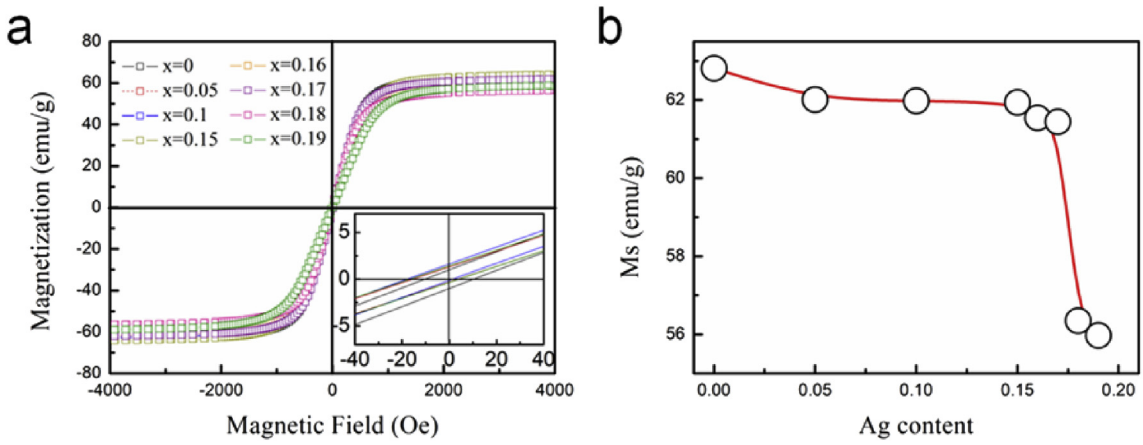

Fig. 6. The magnetic hysteretic loop of the $Li_{1-x}Ag_xFe_5O_8$ ($0 \le x < 0.2$) ceramics in the magnetic field range of -4000-4000 Oe and -40-40 Oe (a), and the relationship between Ag content and the room-temperature magnetization saturation (M_s) as a function of the x value (b).

the changing of the B sites ions concentration has caused the decreasing of magnetization saturation as well as the cut off frequency.

Fig. 6b has shown the relationship between Ag content and the room-temperature magnetization saturation. The magnetization saturation decreased with the Ag content increasing. According to the equation of $B = \mu_0 (H_m + M_s)$, it is concluded that when the permeability has the tendency of increasing the M_s could be down. Compared with Fig. 5a, it could be explained further that the permeability can vary inversely with the magnetization saturation, and a few Ag ions could improve the μ_0 and decrease the M_s simultaneously.

4. Conclusions

In summary, the novel spinel solid solution ceramics $Li_{1-x}Ag_xFe_5O_8$ ($0 \le x < 0.2$) were prepared via solid state reaction method. It is concluded that measuring XRD, SEM, VSM, and HP4291B, the ceramics possess favorable dielectric and magnetic properties, in which the permittivity value reaches about 170 at 200 MHz and meanwhile the real part of permeability attains 47.1 at 20 MHz when Ag^+ doped content is 5%. By coincidence, the density of $Li_{0.95}Ag_{0.05}Fe_5O_8$ acquires the better results that when the sintering temperature is 1170 °C as well. In a word, the $Li_{1-x}Ag_xFe_5O_8$ spinel ferrite with good physical performance obtained in this work might be candidate for novel magneto-dielectric devices.

Acknowledgements

This work was supported by the National Key Research and Development Program of China (2017YFB0406301), the Key Basic Research Program of Shaanxi Province (2017GY-129), the Fundamental Research Funds for the Central University. The SEM work was done at the International Center for Dielectric Research (ICDR), Xi'an Jiaotong University, Xi'an, China and the authors thank Ms. Yan-Zhu Dai for her help in using SEM.

References

[1] Y.M. Dai, Y.F. Wang, C.C. Chen, Synthesis and characterization of magnetic $LiFe_5O_8$-$LiFeO_2$ as a solid basic catalyst for biodiesel production, Catal. Commun. 106 (2018) 20–24.
[2] M. Arillo, M. López, C. Pico, Order-disorder transitions and magnetic behavior in lithium ferrites $Li_{0.5+0.5x}Fe_{2.5-1.5x}Ti_xO_4$ (x = 1.28 and 1.50), Eur. J. Inorg. Chem. 13 (2003) 2397–2405.
[3] L. He, S. Mi, X. Jin, Order-disorder phase transition and magneto-dielectric properties of (1-x)$LiFe_5O_8$-x$Li_2ZnTi_3O_8$ spinel-structured solid solution ceramics, J. Am. Ceram. Soc. 98 (2015) 2122–2129.
[4] M.A. Elkestawy, AC conductivity and dielectric properties of $Zn_{1-x}Cu_xCr_{0.8}Fe_{1.2}O_4$ spinel ferrites, J. Alloys Compd. 492 (2010) 616–620.
[5] P. Zhang, Y. Zhao, Effects of structural characteristics on microwave dielectric properties of $Li_2Mg(Ti_{1-x}Mn_x)_3O_8$ ceramics, J. Alloys Compd. 647 (2015) 386–391.
[6] N. Chen, Y. Yao, D. Wang, $LiFe(MoO_4)_2$ as a novel anode material for lithium-ion batteries, ACS Appl. Mater. Interfaces 6 (2014) 10661–10666.
[7] X. Liu, Y. Lyu, Z. Zhang, Nanotube Li_2MoO_4: a novel and high-capacity material as a lithium-ion battery anode, Nanoscale 6 (2014) 13660–13667.
[8] Y. Liao, F. Xu, D. Zhang, Low temperature firing of $Li_{0.43}Zn_{0.27}Ti_{0.13}Fe_{2.17}O_4$ ferrites with enhanced magnetic properties, J. Am. Ceram. Soc. 98 (2015) 2556–2560.
[9] C.J. Chen, M. Greenblatt, J.V. Waszczak, Lithium insertion compounds of $LiFe_5O_8$, $Li_2FeMn_3O_8$, and $Li_2ZnMn_3O_8$, J. Solid State Chem. 64 (1986) 240–248.
[10] L. He, D. Zhou, F. Xiang, A novel magnetodielectric solid solution ceramic 0.4$LiFe_5O_8$-0.6$Li_2MgTi_3O_8$ with excellent microwave dielectric properties, J. Am. Ceram. Soc. 96 (2013) 3027–3030.
[11] H. Xiang, L. Fang, W. Fang, A novel low-firing microwave dielectric ceramic $Li_2ZnGe_3O_8$ with cubic spinel structure, J. Eur. Ceram. Soc. 37 (2017) 625–629.
[12] L. He, H.B. Yang, D. Zhou, Improved dielectric and magnetic properties of 1-3-type $Ni_{0.5}Zn_{0.5}Fe_2O_4$/epoxy composites for high-frequency applications, J. Phys. D Appl. Phys. 46 (2013) 125003.
[13] C. Boyraz, D. Mazumdar, M. Iliev, Structural and magnetic properties of lithium ferrite ($LiFe_5O_8$) thin films: influence of substrate on the octahedral site order, Appl. Phys. Lett. 98 (2011) 171.
[14] M.N. Iliev, V.G. Ivanov, N.D. Todorov, Lattice dynamics of the α and β phases of $LiFe_5O_8$, Phys. Rev. B 83 (2011) 174111.
[15] Y.P. Fu, Electrical conductivity and magnetic properties of $Li_{0.5}Fe_{2.5-x}Cr_xO_4$ ferrite, Mater. Chem. Phys. 115 (2009) 334–338.
[16] P.B. Braun, A superstructure in spinels, Nature 170 (1952), 1123-1123.
[17] V. Verma, R.K. Kotnala, V. Pandey, The effect on dielectric losses in lithium ferrite by cerium substitution, J. Alloys Compd. 466 (2008) 404–407.
[18] B. Antic, D. Rodic, A.S. Nikolic, The change of crystal symmetry and cation ordering in Li-Mg ferrites, J. Alloys Compd. 336 (2002) 286–291.
[19] L. He, D. Zhou, H.B. Yang, A novel magneto-dielectric solid solution ceramic 0.25$LiFe_5O_8$-0.75$Li_2ZnTi_3O_8$ with relatively high permeability and ultra-low dielectric loss, J. Am. Ceram. Soc. 95 (2012) 3732–3734.
[20] L. He, D. Zhou, H.B. Yang, Low-temperature sintering Li_2MoO_4/$Ni_{0.5}Zn_{0.5}Fe_2O_4$ magneto-dielectric composites for high-frequency application, J. Am. Ceram. Soc. 97 (2014) 2552–2556.
[21] Y. Lin, X. Liu, H. Yang, Low temperature sintering of laminated $Ni_{0.5}Ti_{0.5}NbO_4$-$Ni_{0.8}Zn_{0.2}Fe_2O_4$ composites for high frequency applications, Ceram. Int. 42 (2016) 11265–11269.
[22] H.B. Yang, H. Wang, L. He, Polarization relaxation mechanism of $Ba_{0.6}Sr_{0.4}TiO_3$/$Ni_{0.8}Zn_{0.2}Fe_2O_4$ composite with giant dielectric constant and high permeability, J. Appl. Phys. 108 (2010) 4105.
[23] B. Banov, A. Momchilov, M. Massot, Lattice vibrations of materials for lithium rechargeable batteries V Local structure of $Li_{0.3}MnO_2$, Mater. Sci. Eng., B 100 (2003) 87–92.
[24] C.L. Huang, C.H. Su, C.M. Chang, High Q microwave dielectric ceramics in the $Li_2(Zn_{1-x}A_x)Ti_3O_8$, (A = Mg, Co; x = 0.02-0.1) system, J. Am. Ceram. Soc. 94 (2011) 4146–4149.
[25] X.G. Lu, G.Y. Liang, Y.M. Zhang, W. Zhang, Synthesis of $FeNi_3$/$(Ni_{0.5}Zn_{0.5})Fe_2O_4$ nanocomposite and its high frequency complex permeability,

Nanotechnology 18 (2007) 715701.
[26] V. Verma, R.K. Kotnala, V. Pandey, The effect on dielectric losses in lithium ferrite by cerium substitution, J. Alloys Compd. 466 (2008) 404–407.
[27] H. Yang, H. Wang, X. Feng, Microstructure and electromagnetic properties of $SrTiO_3/Ni_{0.8}Zn_{0.2}Fe_2O_4$ composites by hybrid process, J. Am. Ceram. Soc. 92 (2009) 2005–2010.

Jing Li, Di Zhou*
Electronic Materials Research Laboratory, Key Laboratory of the Ministry of Education & International Center for Dielectric Research, School of Electronic and Information Engineering, Xi'an Jiaotong University, Xi'an 710049, China

* Corresponding author.
E-mail address: zhoudi1220@gmail.com (D. Zhou).

24 October 2018
10 January 2019
12 January 2019
Available online 14 January 2019